JCS ePress online publication date 9 December 2008

Spatial organization of nucleotide excision repair proteins after UV-induced DNA damage in the human cell nucleus

Liliana Solimando[1,*,‡], Martijn S. Luijsterburg[2,*,§], Lorella Vecchio[1,*], Wim Vermeulen[3], Roel van Driel[2,¶] and Stanislav Fakan[1]

[1]Centre of Electron Microscopy, University of Lausanne, 27 Bugnon, CH-1005 Lausanne, Switzerland
[2]Swammerdam Institute for Life Sciences, University of Amsterdam, Kruislaan 318, 1098 SM Amsterdam, The Netherlands
[3]Department of Cell Biology and Genetics, Medical Genetics Center, Erasmus Medical Center, P.O. Box 1738, 3000 DR Rotterdam, The Netherlands

*These authors contributed equally to this work
‡Current address: Department of Cell and Molecular Biology, Feinberg School of Medicine, Northwestern University 303 E. Chicago Avenue, Ward Building W11-145, Chicago, IL 60611, USA
§Current address: Department of Cell and Molecular Biology, The Karolinska Institute, von Eulers väg 3, S-17177 Stockholm, Sweden
¶Author for correspondence (e-mail: r.vandriel@uva.nl)

Accepted 25 September 2008
Journal of Cell Science 122, 83-91 Published by The Company of Biologists 2009
doi:10.1242/jcs.031062

Summary

Nucleotide excision repair (NER) is an evolutionary conserved DNA repair system that is essential for the removal of UV-induced DNA damage. In this study we investigated how NER is compartmentalized in the interphase nucleus of human cells at the ultrastructural level by using electron microscopy in combination with immunogold labeling. We analyzed the role of two nuclear compartments: condensed chromatin domains and the perichromatin region. The latter contains transcriptionally active and partly decondensed chromatin at the surface of condensed chromatin domains. We studied the distribution of the damage-recognition protein XPC and of XPA, which is a central component of the chromatin-associated NER complex. Both XPC and XPA rapidly accumulate in the perichromatin region after UV irradiation, whereas only XPC is also moderately enriched in condensed chromatin domains. These observations suggest that DNA damage is detected by XPC throughout condensed chromatin domains, whereas DNA-repair complexes seem preferentially assembled in the perichromatin region. We propose that UV-damaged DNA inside condensed chromatin domains is relocated to the perichromatin region, similar to what has been shown for DNA replication. In support of this, we provide evidence that UV-damaged chromatin domains undergo expansion, which might facilitate the translocation process. Our results offer novel insight into the dynamic spatial organization of DNA repair in the human cell nucleus.

Supplementary material available online at
http://jcs.biologists.org/cgi/content/full/122/1/83/DC1

Key words: DNA repair, Chromatin, Nuclear organization, Nucleotide excision repair

Introduction

Nucleotide excision repair (NER) is a highly conserved DNA repair system that removes a variety of damage from the genome (Hoeijmakers, 2001). Placental mammals fully rely on NER for the removal of UV-induced lesions, such as cyclobutane pyrimidine dimers (CPDs) and 6-4 photoproducts (6-4 PPs). Both types of helix-distorting lesions are potent inhibitors of transcription by RNA polymerase II (RNAP II) and replication by DNA polymerases δ and ε (Lehmann et al., 2007). Two closely related NER pathways exist that are referred to as global genome NER (GGR) and transcription-coupled NER (TCR). TCR removes lesions exclusively from transcribed genes, whereas GGR repairs lesions elsewhere in the genome (Hanawalt, 2002). Damage recognition in GGR is carried out by the XPC protein complex, which subsequently recruits the repair machinery to process the lesions (Araki et al., 2001; Buterin et al., 2005; Maillard et al., 2007; Sugasawa et al., 1998; Volker et al., 2001). DNA damage in actively transcribed genes is detected by a stalled RNAP II in concert with the CSA and CSB proteins, which are essential for TCR (Brueckner and Cramer, 2007; Fousteri et al., 2006; Hanawalt, 2000; Laine and Egly, 2006). Although CPDs are more abundant than 6-4 PPs following UV irradiation, the latter photoproduct is removed approximately five times faster than CPDs (Mitchell and Nairn, 1989). CPD removal by GGR is inefficient, probably because of the lower affinity of XPC for this type of lesion. For the recognition of CPDs in GGR, XPC is assisted by UV-damaged DNA-binding protein complex (UV-DDB; comprised of DDB1 and DDB2), which is essential for efficient repair of CPDs (Groisman et al., 2003; Hwang et al., 1998; Tang et al., 2000). TCR is particularly important for the removal of lesions, such as CPDs, that are inefficiently cleared away by GGR (Balajee and Bohr, 2000; Hanawalt, 2000; Mullenders and Berneburg, 2001). After the damage-recognition step in GGR and TCR, both pathways converge to a common molecular mechanism that involves approximately 30 proteins in mammals (Araujo et al., 2000; de Laat et al., 1999; Lindahl and Wood, 1999). The ten-subunit protein complex TFIIH is the first to be recruited to the damaged DNA after the recognition step by XPC or CSB (Fousteri et al., 2006; Giglia-Mari et al., 2004; Volker et al., 2001; Yokoi et al., 2000). TFIIH uses its XPD helicase subunit to unwind the DNA around a lesion (Coin et al., 2007). The XPA protein is a central organizer of the NER complex and is involved in the proper orientation of the incision proteins XPG and ERCC1-

XPF together with RPA (de Laat et al., 1998; Missura et al., 2001). Following dual incision by the two NER endonucleases, a stretch of ~30 nucleotides is released, after which DNA polymerase δ is loaded by PCNA and fills the remaining gap, which is subsequently sealed by XRCC1-ligase III (de Laat et al., 1999; Hoeijmakers, 2001; Lindahl and Wood, 1999; Moser et al., 2007). After repair synthesis and ligation, CAF1 (also known as CNOT7) is recruited to the repair site to deposit new histones and re-establish the chromatin state (Green and Almouzni, 2003; Polo et al., 2006).

Although NER has been studied extensively in vitro and in vivo, we are beginning to understand the kinetics (i.e. temporal organization) of the assembly of the NER complex on a chromatin template in nuclei of living cells. However, little is known about the spatial organization of DNA repair in the nucleus. It has been known for many years that the cell nucleus is a highly compartmentalized structure that contains distinct structural domains. For example, the nucleus contains chromatin-dense subchromosomal domains of about 100-500 nm that are surrounded by interchromatin space that contains little or no chromatin (Cremer et al., 2004). Each dense chromatin domain contains several Mbs of DNA and a chromosome consists of a number of these dense chromatin domains. The perichromatin region, constituting a shell of partly decondensed chromatin at the surface of condensed chromatin domains, is a nuclear domain where replication and transcription mainly take place (Cmarko et al., 1999; Fakan, 1994; Fakan and van Driel, 2007; Jaunin and Fakan, 2002). Newly replicated DNA in the perichromatin region is rapidly internalized into the condensed chromatin area (Jaunin et al., 2000). Polycomb (PcG) proteins are also concentrated in this compartment, suggesting that PcG-mediated silencing also occurs mainly at the periphery of condensed chromatin (Cmarko et al., 2003).

In this study we investigated where NER occurs in the nucleus of human cells. Our results indicate that the NER proteins XPC and XPA become significantly enriched in the perichromatin region after global UV-C irradiation. This suggests that NER predominantly takes place in the same chromatin compartment in which transcription and replication occur. In addition, we provide evidence for considerable chromatin decondensation in response to UV-induced DNA damage, which might facilitate relocation of DNA lesions to the perichromatin region. Together, our results provide novel insight into the dynamic spatial organization of DNA repair in the human cell nucleus.

Results

Visualization of DNA damage and NER proteins by fluorescence microscopy

To study whether DNA repair by NER is compartmentalized in the human nucleus or if it occurs throughout the genome, we have analyzed the nuclear distribution of the NER proteins XPC and XPA before and after UV-C irradiation at the ultrastructural level by immunogold labeling on ultrathin sections. To this aim, we generated cell lines stably expressing XPC-EGFP and EGFP-XPA (Hoogstraten et al., 2008; Rademakers et al., 2003). The fusion proteins were expressed in human repair-deficient XP4PA-SV and XP2OS-SV cells, lacking functional XPC and XPA, respectively. Expression of the fusion proteins re-established UV resistance of the cell lines, showing that the EGFP-tagged NER proteins are functional (Hoogstraten et al., 2008; Rademakers et al., 2003). Moreover, the nuclear concentration of the fusion proteins was similar to that of the endogenous proteins in wild-type cells (Hoogstraten et al., 2008; Rademakers et al., 2003). We analyzed the subnuclear distribution of EGFP-tagged NER proteins rather than that of the endogenous proteins because antibodies against the latter did not recognize their antigens after embedding and sectioning. By contrast, anti-GFP antibodies did work well under these conditions. Fig. 1D,H and Fig. 1F,H show that, in formaldehyde-fixed cells that are analyzed by light microscopy, anti-EGFP antibody labeling shows precisely the same intranuclear distribution as the intrinsic fluorescence of XPC and XPA in cells that express XPC-EGFP and EGFP-XPA, respectively. This validates the use of anti-EGFP antibodies in our studies.

Cells expressing XPC-EGFP and EGFP-XPA were UV-C irradiated (60 $J.m^{-2}$) and subsequently immunolabeled for CPDs, using an anti-CPD antibody (Fig. 1A,D) (Mori et al., 1991). Whereas hardly any signal was detected in control cells, irradiated cells showed a nuclear signal in every cell (Fig. 1A,D), confirming that significant numbers of CPDs are produced under these conditions. Confocal microscopy showed that, within the resolution of light microscopy, the distribution of EGFP-XPA is homogeneous throughout the nucleus in UV-irradiated and control cells (Fig. 1E). By contrast, XPC-EGFP displayed a typical chromatin-like distribution in irradiated and control cells (Fig. 1B). This is probably due to the affinity of this protein for DNA in general (Shivji et al., 1994). Global UV-C irradiation did not result in a visible redistribution of these two repair proteins at the light-microscopic level (Fig. 1B,E). To show that XPC and XPA are engaged in NER after UV-C irradiation, we performed strip-FRAP (Houtsmuller and Vermeulen, 2001) on globally irradiated cells and control cells. Significant immobilization of XPC-EGFP (Fig. 1G) and of EGFP-XPA (Fig. 1H) was detected after UV-C irradiation, indicating that a significant fraction of both protein pools participates in DNA repair under our experimental conditions (see also Rademakers et al., 2003).

Ultrastructural distribution of UV-induced DNA lesions

To analyze the spatial distribution of UV-induced DNA lesions upon global UV-C irradiation, we used immunogold labeling of ultrathin sections with antibodies that specifically bind to CPDs (Mori et al., 1991). In order to obtain optimal immunocytochemical reactivity, cells were fixed only with paraformaldehyde, in accordance with a number of previously reported experiments (Cmarko et al., 1999; Cmarko et al., 2003; Jaunin et al., 2000). Fraschini et al. have shown that nuclear morphology of lymphocytes, as observed on ultrathin sections after conventional staining or using the EDTA method, is similar when comparing formaldehyde-fixed and glutaraldehyde-fixed cells (Fraschini et al., 1981). We discriminate between two nuclear compartments: condensed chromatin domains and the perichromatin region. The former are defined as nuclear areas that are relatively weakly contrasted by the EDTA regressive staining method. The perichromatin region is operationally defined as an approximately 80-nm-wide shell at the surface of condensed chromatin domains. From the approximate size of the EGFP molecule and the primary and secondary antibody, it can be estimated that the gold particle is located somewhere in a sphere of 40 nm around the antigen. Therefore, this definition includes antigens up to about 80 nm at both sides of the surface of condensed chromatin domains, including those in dispersed chromatin and RNP-containing structures, such as perichromatin fibrils and granules, near the surface.

Global UV irradiation at 60 $J.m^{-2}$ resulted in a significant increase in CPD labeling density in the perichromatin region and condensed chromatin domains compared with non-irradiated control cells,

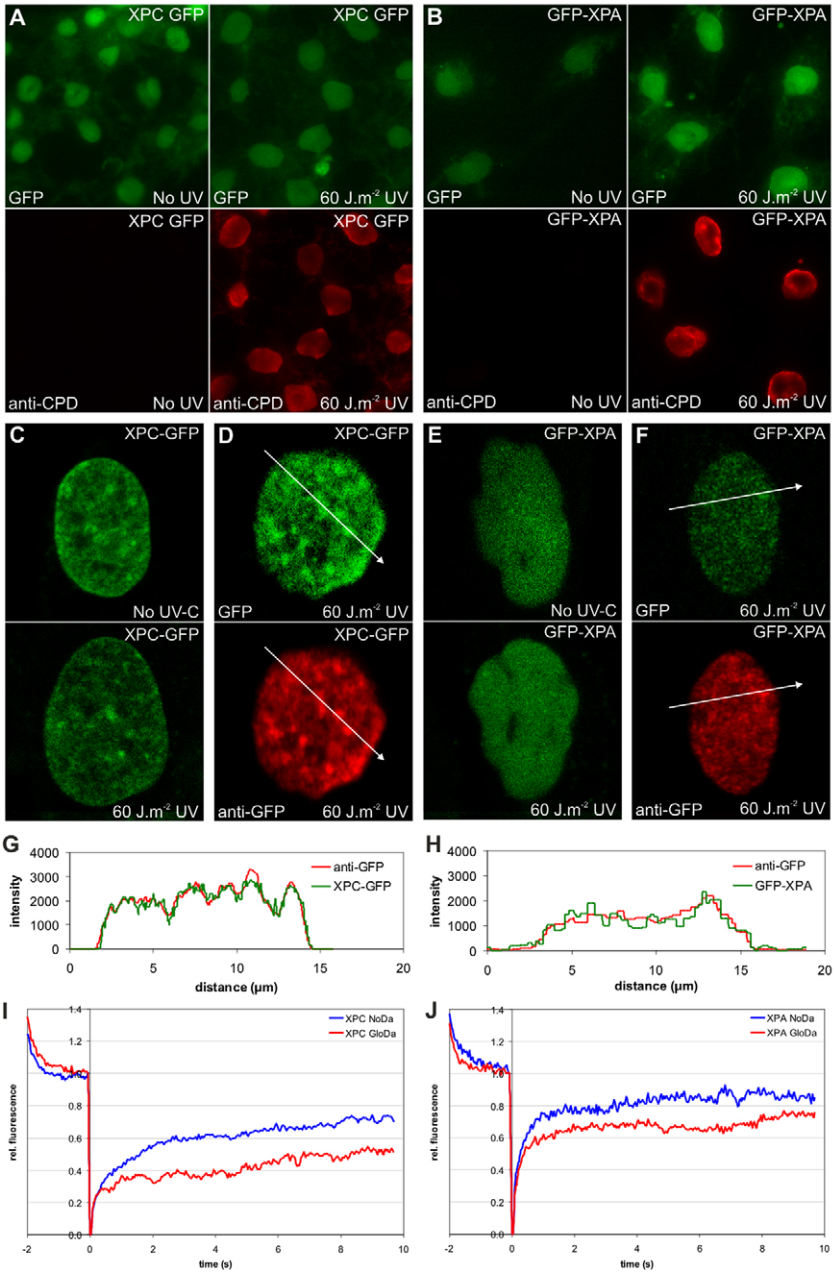

Fig. 1. Immunofluorescence and live-cell microscopy. (A,B) Example of XPC-EGFP (A) and EGFP-XPA (B) cells immunofluorescently labeled against CPDs in non-irradiated control cells (left panels) or 10 minutes after global UV-C irradiation at 60 J.m^{-2} (right panels). The EGFP signal is shown in green (upper panels) and the anti-CPD staining of the same cells in red (lower panels). (C) Confocal slice of living XPC-EGFP cells either non-irradiated (upper panel) or globally irradiated at 60 J.m^{-2} (lower panel). (D) Confocal slice of XPC-EGFP cells immunofluorescently labeled against EGFP in cells 10 minutes after global UV-C irradiation at 60 J.m^{-2}. The intrinsic EGFP signal is shown in green (upper panel) and the anti-EGFP staining of the same cell in red (lower panel). (E) Confocal slice of living EGFP-XPA cells either non-irradiated (upper panel) or globally irradiated at 60 J.m^{-2} (lower panel). (F) Confocal slice of EGFP-XPA cells immunofluorescently labeled against EGFP in cells 10 minutes after global UV-C irradiation at 60 J.m^{-2}. The intrinsic EGFP signal is shown in green (upper panel) and the anti-EGFP staining of the same cell in red (lower panel). (G) Line scan of the arrows depicted in the upper and lower panels of D, reflecting intrinsic XPC-GFP fluorescence (green line) and anti-EGFP signal (red line) in the same cell. (H) Line scan of the arrows depicted in the upper and lower panels of F, reflecting intrinsic EGFP-XPA fluorescence (green line) and anti-EGFP signal (red line) in the same cell. (I) FRAP analysis of XPC-EGFP in non-irradiated cells (blue line, *n*=9) or globally irradiated cells at 60 J.m^{-2} (red line, *n*=9). (J) FRAP analysis of EGFP-XPA in non-irradiated cells (blue line, *n*=9) or globally irradiated cells at 60 J.m^{-2} (red line, *n*=9).

showing that CPDs are present throughout these two nucleoplasmic domains (Fig. 2). Quantitative analysis of the CPD distribution in condensed chromatin domains and the perichromatin region (defined as an approximately 80-nm-wide shell at the surface of condensed chromatin domains) shows that the perichromatin region is labeled half as much as condensed chromatin domains (Fig. 5A). This is most likely due to the fact that chromatin in the perichromatin region is more unfolded compared with condensed chromatin domains (Bouchet-Marquis et al., 2006) (for reviews, see Fakan, 2004a; Fakan and van Driel, 2007). These results show that the perichromatin region contains an approximate 50% lower concentration of DNA lesions compared with dense chromatin domains. Assuming that the probability of UV-induced DNA damage is the same in both compartments, this indicates an approximate 50% lower concentration of chromatin in the perichromatin region compared with condensed chromatin domains.

Ultrastructural distribution of protein factors involved in NER

To establish whether DNA repair by NER occurs in specific nuclear regions, we analyzed the distribution of EGFP-XPA and XPC-EGFP using anti-EGFP antibodies in non-irradiated cells or after 10 minutes and 60 minutes following global UV-C irradiation (60 J.m^{-2}). After UV irradiation, the labeling intensity of XPA in condensed chromatin domains slightly decreased (Fig. 3A,B and Fig. 5C), whereas XPC accumulated about 1.5-fold more compared with non-irradiated cells (Fig. 3C,D and Fig. 5C). The UV-induced accumulation of both proteins in the perichromatin region was between three- and six-fold, which is considerably higher than the accumulation in condensed chromatin domains (Fig. 5B). Since the average chromatin density in the perichromatin region was about 50% lower than in condensed chromatin domains, as can be inferred from the difference in CPD labeling (see above), this shows that these two NER proteins accumulate (per unit chromatin) about tenfold more in the

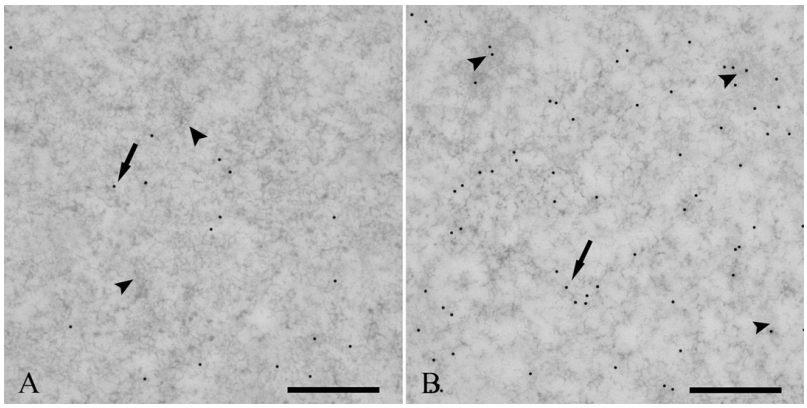

Fig. 2. Ultrastructural localization of CPDs. Example of a human XP2OS-SV fibroblast, immunolabeled using a specific antibody against CPDs, that has been (A) mock treated and (B) fixed 10 minutes after global UV-C irradiation at 60 J.m^{-2}. Samples were contrasted with the EDTA regressive technique in order to reduce the contrast of chromatin. Arrowheads indicate condensed chromatin; arrows designate the perichromatin region. Scale bars: 0.5 µm.

perichromatin region than in condensed chromatin in response to UV damage. This indicates that about one order of magnitude more pre-incision complexes are assembled in the perichromatin region than in compact chromatin domains after UV irradiation. There is no systematic difference between the labeling at 10 minutes and at 60 minutes after UV irradiation (Fig. 5B,C), indicating that the preferential accumulation in the perichromatin region is not due to, for instance, slow diffusion of proteins into the condensed chromatin domain. Our results indicate that assembly of pre-incision complexes preferentially takes place in the perichromatin region, suggesting that this is the site where NER mainly takes place.

Expansion of condensed chromatin domains after DNA damage

To establish whether UV irradiation results in detectable changes in large-scale chromatin structure, we analyzed ultrathin sections of UV-irradiated cells using osmium ammine, a Feulgen-type stain specifically visualizing DNA (Fig. 4A,B). Quantitative evaluation of the surface area of chromatin domains showed that their surface area increases about twofold after UV irradiation, compared with non-irradiated cells, indicating that the increase in volume of the chromatin domains after UV irradiation is about threefold (Fig. 5D). This is particularly visible in cells fixed 10 minutes after irradiation, whereas, after 60 minutes, the increase is somewhat less, probably due to partial repair of the damaged DNA sites (Fig. 5D). The increase in the volume indicates that, after UV irradiation, chromatin is transiently de-compacted.

Discussion

The results presented in this study indicate that assembly of NER complexes in human cells takes place predominantly in the perichromatin region, an approximately 100-nm-wide area on the

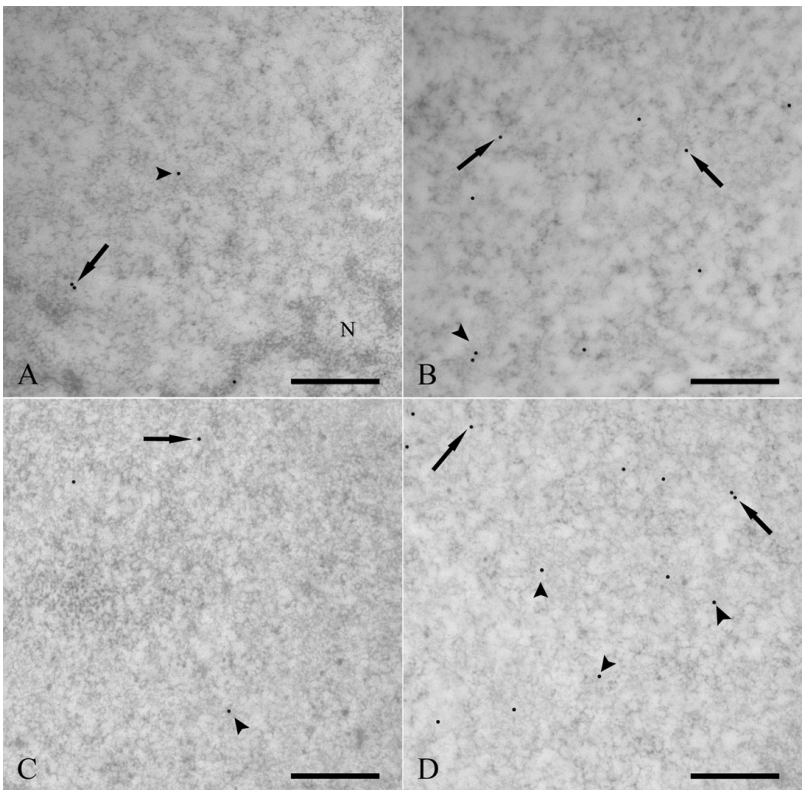

Fig. 3. Ultrastructural localization of EGFP-XPA and XPC-EGFP using anti-EGFP antibodies in non-irradiated and UV-irradiated cells. (A) An example of an XP2OS-SV EGFP-XPA-expressing fibroblast that has been mock treated. (B) A nucleus globally irradiated with UV-C at 60 J.m^{-2}. (C,D) Similarly, an XP4PA-SV XPC-EGFP-expressing cell that was mock treated (C) and a UV-C irradiated cell nucleus (D) are shown. The shown examples were fixed 10 minutes following UV irradiation. Cell monolayers were fixed in paraformaldehyde and thin sections were subsequently immunolabeled with antibodies specific for EGFP. Samples were contrasted with the EDTA regressive technique in order to reduce the contrast of chromatin. The arrows designate the perichromatin region and the arrowheads designate condensed chromatin domains. N, nucleolus. Scale bars: 0.5 µm.

border of compact chromatin domains in the interphase nucleus (Fakan and van Driel, 2007). Transcription and replication have also been shown to be concentrated in this nuclear region (Cmarko et al., 1999; Fakan, 2004b; Fakan and van Driel, 2007; Jaunin and Fakan, 2002; Jaunin et al., 2000). We used immuno-electron microscopy to identify the spatial distribution of UV-induced lesions (CPDs) and two core NER proteins, i.e. the NER damage-recognition protein XPC and the NER protein XPA, which play a crucial role in damage verification and regulation of dual incision during NER (Missura et al., 2001; Sugasawa et al., 1998; Volker et al., 2001). By using cell lines that stably express fluorescent-protein-tagged XPC and XPA (XPC-EGFP and EGFP-XPA), we carried out light- and electron-microscopic studies in parallel. The light-microscopic observations support the electron-microscopic data, as far as the resolution of the former allows. FRAP experiments show that, after global UV-C irradiation, a substantial fraction of the XPC and XPA molecules is bound to UV-damaged chromatin (Fig. 1). High-resolution electron-microscopic analysis revealed that accumulation of repair factors occurs preferentially in the perichromatin region, suggesting that this is the main site of assembly of the NER protein complex (Fig. 3 and Fig. 5B).

The distribution of XPC at the light-microscopic level is similar to that of chromatin in non-irradiated cells (Fig. 1B), reflecting its affinity for undamaged DNA (Shivji et al., 1994; Sugasawa et al., 1998). By contrast, XPA is diffusely distributed throughout the nucleoplasm (Fig. 1E) (Rademakers et al., 2003). As expected, immunogold labeling shows that, after UV irradiation, CPDs are present throughout the condensed chromatin domains and in the perichromatin region (Fig. 2 and Fig. 5A) (Gazave et al., 2005). The concentration of damage-recognition protein XPC in the condensed chromatin domains increases about twofold in the first 10 minutes after UV exposure, most probably reflecting its binding to 6-4 PPs (Fig. 5B). In agreement with this notion, live-cell experiments have shown that, under these experimental conditions, a maximal amount of the XPC protein pool (~25%) is bound to damaged DNA (Hoogstraten et al., 2008). Given the fact that, in these cells, roughly 20% of the nucleus is occupied by condensed chromatin domains (Fig. 4 and Fig. 5D), we can estimate that a two- to three-fold increase in XPC concentration in condensed chromatin domains after global UV irradiation can be expected, which is also what we measure (see Materials and Methods). No significant increase in XPA binding in condensed chromatin domains was observed, despite the fact that, under these conditions, about 30% of the XPA molecules are bound to damaged DNA sites (Rademakers et al., 2003). By contrast, both XPC and XPA accumulate between three- and six-fold in the perichromatin region after UV irradiation (Fig. 5B). This is an underestimate of the real accumulation per unit chromatin, because chromatin in the perichromatin region is more decondensed, resulting in a lower local chromatin concentration. Assuming that the CPD concentration is a crude measure for the chromatin concentration, we found that the chromatin concentration in condensed chromatin domains after UV irradiation is about twofold higher compared with that in the perichromatin region (Fig. 5A). This indicates a tenfold increase in XPC and XPA binding per unit chromatin in the perichromatin region. Therefore, our results reveal that at least one order of magnitude more pre-incision NER complexes are assembled in this sub-chromosomal region in response to UV damage than in condensed chromatin domains. XPC accumulation in condensed chromatin after UV irradiation is considerably lower than in the perichromatin region (~ twofold enrichment compared with non-irradiated cells), whereas no enrichment of XPA is detected in condensed chromatin after UV irradiation. Since XPC is exclusively involved in GGR (van Hoffen et al., 1995), our results suggest that

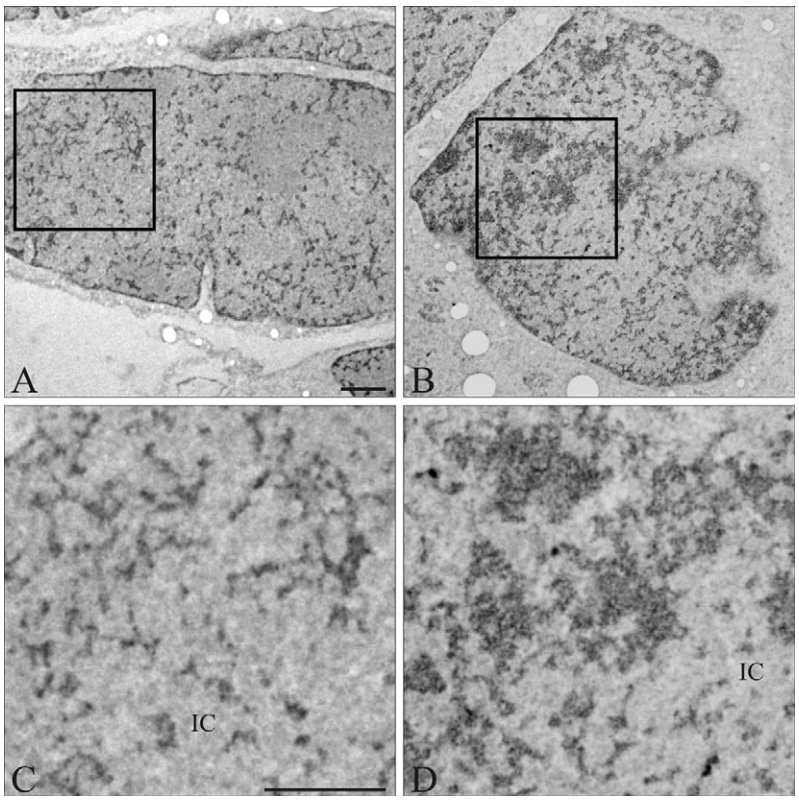

Fig. 4. Increase in the amount of dense chromatin areas upon global UV-C irradiation. XP2OS-SV EGFP-XPA-expressing cells were (A,C) mock treated or (B,D) fixed 10 minutes after global UV irradiation at 60 $J.m^{-2}$, and subsequently stained with osmium ammine to specifically visualize DNA (dark color). The analyzed sections were collected at the middle nuclear plane of the cells. C and D represent close-ups of the boxed areas in A and B, respectively. IC, interchromatin compartment. Scale bars: 1.25 μm.

GGR predominantly takes place in the perichromatin region. As most transcription takes place in the perichromatin region, it might be expected that transcription-coupled NER also occurs in this region. During the first 60 minutes after UV irradiation, the concentration of damaged sites hardly decreased (Fig. 5A). Since, under our experimental conditions, the number of UV-induced DNA lesions is high compared with the number of available NER proteins, one does indeed expect only a moderate decrease in the number of CPDs (Moser et al., 2005; van Hoffen et al., 1995). The counts of immunogold particles in perichromatin and condensed chromatin, on which the histograms in Fig. 5 are based, are presented as supplementary material Table S1.

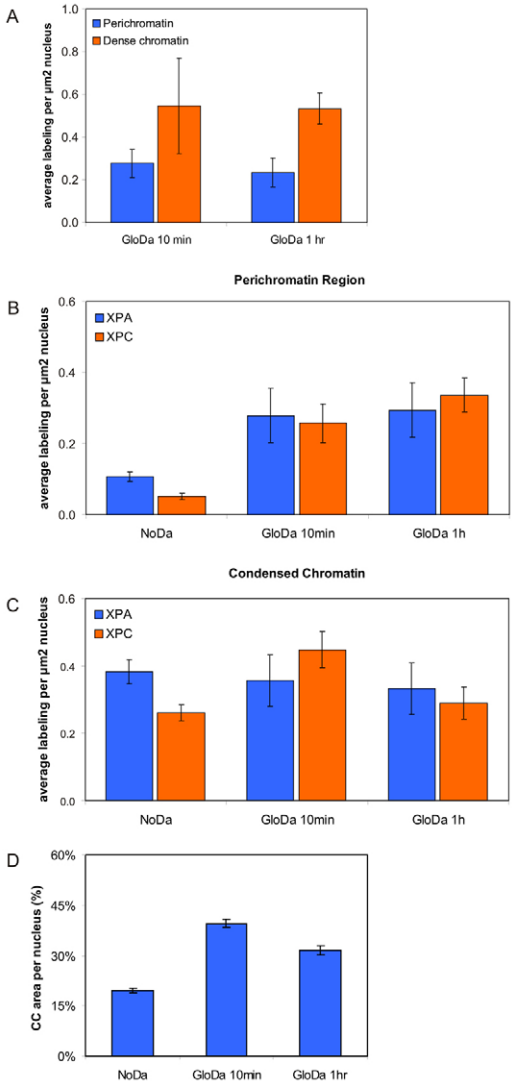

Fig. 5. Quantitative evaluations of ultrastructural data. (A) A quantitative evaluation of CPD labeling density in irradiated cells either 10 minutes (n=10) or 1 hour (n=10) following irradiation in condensed chromatin domains (orange bars) and the perichromatin region (blue bars). Values were corrected for residual labeling in non-irradiated cells (n=20). The values represent the average gold-grain number per μm^2 nuclear surface area ± s.e.m. (B,C) A quantitative evaluation of EGFP-XPA (blue bars) and XPC-EGFP (orange bars) labeling density (gold particles per μm^2 nuclear area) in the perichromatin region (B) or in condensed chromatin domains (C). The labeling density was determined in non-irradiated cells (n=20 for XPC and XPA; NoDa), and in nuclei 10 minutes (n=15 for XPC and XPA) and 1 hour (n=15 for XPC and XPA) following irradiation. Values represent the average ± s.e.m. (D) A quantitative evaluation of the fraction of the nucleus occupied by condensed chromatin domains (%) before (n=29; NoDa) and after global UV irradiation at 60 $J.m^{-2}$ determined 10 minutes (n=15) or 1 hour (n=15) following UV exposure. The values represent the mean ± s.e.m. NoDa, no UV irradiation; GloDa, after global UV irradiation.

Our results suggest that UV-induced DNA lesions are detected by XPC throughout the condensed chromatin domains, but that the pre-incision NER complex is assembled predominantly in the perichromatin region, i.e. at or near the surface of the condensed chromatin domains. It is tempting to speculate that damaged sites are translocated to the surface of condensed chromatin domains. Although the mechanism of this process is not known, it might be the same as that used for relocating replicating DNA transiently to the perichromatin region and newly synthesized DNA back into the condensed chromatin domain (Jaunin et al., 2000). If lesions are indeed translocated to the perichromatin region, this might explain in part why TCR is much faster than GGR (Bohr et al., 1985; Mellon et al., 1987), because active genes are predominantly located in the perichromatin area and do not need translocation. We observe an about threefold increase in volume of chromatin domains after UV irradiation, reflecting a considerable overall de-compaction. It is attractive to speculate that this chromatin expansion is required for the relocation of damaged chromatin. Other studies have suggested similar chromatin decondensation related to UV-induced DNA damage and to the formation of double-strand breaks (Carrier et al., 1999; Kruhlak et al., 2006; Murga et al., 2007; Rubbi and Milner, 2003; Wang et al., 2006; Ziv et al., 2006). Chromatin decondensation in response to UV irradiation has been suggested to depend on p53 (Rubbi and Milner, 2003), the small acidic GADD45 protein (Carrier et al., 1999) and members of the ING tumor-suppressor family (Kuo et al., 2007; Wang et al., 2006). Chromatin decondensation thus seems a general response to DNA damage that is triggered by DNA-damage response processes other than DNA repair.

Together, our study provides novel insight into the spatial organization of the DNA-repair process by NER. Major changes in chromatin structure seem to occur after the detection of UV-damaged sites. It might be that these changes in chromatin structure facilitate the translocation of damaged DNA sites to the perichromatin region. The molecular mechanism of this process is unclear. It probably involves binding of XPC, which shows a significant accumulation inside condensed chromatin domains after UV irradiation. Alternatively, the UV-DDB protein complex, which is required for CPD repair and binds rapidly to UV-induced DNA lesions (Dualan et al., 1995; Luijsterburg et al., 2007; Takao et al., 1993), might be involved. Although much less efficiently than in wild-type cells, XPC binds to 6-4 PPs in XP-E cells (UV-DDB deficient), indicating that DDB2 is not an absolute prerequisite for XPC binding to this particular type of lesion (Moser et al., 2005). DDB2 is crucial for the recognition and repair of CPDs, and overexpression of DDB2 leads to enhanced recruitment of XPC to CPDs (Fitch et al., 2003). It is conceivable that UV-DDB is required to facilitate translocation of CPDs to the perichromatin region.

This study, together with previous work, establishes that major chromatin-associated processes, such as transcription, replication, Polycomb-mediated gene silencing and DNA repair, preferentially occur at the interface between condensed chromatin domains and the interchromatin space, i.e. the perichromatin region. They raise the fundamental question, what mechanisms are involved in translocating DNA lesions to the perichromatin region and probably

back again into condensed chromatin domains after repair? It is likely that it is similar to the mechanism responsible for the movement of replicating DNA. Together, our results add a spatial dimension to our understanding of NER in the human cell nucleus, revealing that the spatiotemporal organization of an essential chromatin-association process is more complex than anticipated.

Materials and Methods

Cell lines and culture conditions

Cell lines used in this study were human XPC-deficient fibroblasts (XP4PA-SV) expressing XPC-EGFP (Hoogstraten et al., 2008) and human XPA-deficient fibroblasts (XP2OS-SV) expressing EGFP-XPA (Rademakers et al., 2003). The cell lines were cultured in a 1:1 mixture of DMEM:Ham's F10 medium. All media contained glutamine (Gibco, Breda, The Netherlands) and were supplemented with antibiotics and 10% FCS, and all cells were cultured at 37°C in an atmosphere of 5% CO_2.

Global UV-C irradiation

For all experiments, cells were irradiated with a UV-C source containing four UV lamps (TUV 9W PL-S; Philips, Eindhoven, The Netherlands). The UV dose rate was 1.48 $W.m^{-2}$ at 254 nm as measured with an SHD 240/W detector connected to an IL 1700 radiometer (International Light Technologies, Peabody, MA). For induction of global UV-C damage, cells were rinsed with phosphate buffered saline (PBS) and irradiated for 40 seconds, resulting in a UV dose of 60 $J.m^{-2}$. Control cells were mock treated.

Immunolabeling for fluorescence microscopy

Cells were fixed with 4% formaldehyde in PBS for 15 minutes at 4°C, permeabilized in 0.5% Triton X-100 (Serva, Heidelberg, Germany) in PBS for 5 minutes, and incubated with 80 mM glycine in PBS for 10 minutes to block unreacted aldehyde groups. Cells were rinsed with PB (130 mM KCl, 10 mM Na_2HPO_4 and 2.5 mM $MgCl_2$, pH 7.4) and equilibrated in WB [PB containing 0.5% bovine serum albumin (BSA), 0.2% gelatin and 0.05% Tween 20; Sigma-Aldrich, St Louis, MO]. Antibody steps and washes were in WB. EGFP labeling was carried out using a rabbit polyclonal antibody (Ab) against EGFP (1:5000; Eusera, Edmonton, Alberta, Canada) and detection was by donkey anti-rabbit Ig coupled to Cy3 (1:500; Jackson ImmunoResearch Laboratories, West Grove, PA).

Immunolabeling of CPDs was performed using mouse monoclonal Ab TDM-2 (Mori et al., 1991). For this, the above steps were repeated but, prior to labeling, DNA was denatured with 2 M HCl for 30 minutes at 37°C and blocked in 10% BSA in PB for 15 minutes. Detection was done using donkey anti-mouse Ig coupled to Cy3 (1:500; Jackson ImmunoResearch Laboratories). Samples were mounted in Vectashield (Vector Laboratories, Burlingame, CA).

Fluorescence microscopy

Fluorescence microscopy was performed on a Zeiss Axiovert 200M wide-field fluorescence microscope, equipped with a 100× Plan-Apochromat (1.4 NA) oil-immersion lens (Zeiss, Oberkochen, Germany) and a Cairn Xenon Arc lamp with monochromator (Cairn Research, Kent, UK). Images were recorded with a cooled CCD camera (Coolsnap HQ, Roper Scientific, USA). A 375-490 excitation filter, 490 dichroic mirror and 525-40 band-pass emission filter was used for EGFP imaging (monochromator: 470 nm ± 20 nm), and a 375-580 excitation filter, 585 dichroic mirror and 620-60 band-pass emission filter was used for Cy3 imaging (monochromator: 550 nm ± 20 nm). Confocal fluorescence microscopy was performed on a Zeiss LSM 510 confocal microscope, equipped with a 63× Plan-A (1.4 NA) oil-immersion lens (Zeiss, Oberkochen, Germany) and a 60 mW Argon laser (488 and 514 nm).

Fluorescence recovery after photobleaching (FRAP)

FRAP analysis was used to measure the mobility of XPC-EGFP and EGFP-XPA as described by Houtsmuller and co-workers (Hoogstraten et al., 2002; Houtsmuller et al., 1999; Rademakers et al., 2003; Zotter et al., 2006). Briefly, a strip of 512×50 pixels was imaged with 38 ms per frame at zoom 8 (1 pixel is 0.04 μm by 0.04 μm). After 5-8 images, a strip of 512×40 pixels was bleached by applying five scans at maximal 488 nm and 514 nm laser intensity (AOTF 100%, total time 160 ms) and the fluorescence recovery was acquired by scanning at least 100 images. The data was corrected for background fluorescence and normalized to pre-bleach intensity. FRAP experiments were performed on a Zeiss LSM 510 confocal microscope, equipped with a 63× Plan-A (1.4 NA) oil-immersion lens (Zeiss, Oberkochen, Germany) and a 60 mW Argon laser (488 and 514 nm). The LSM510 was equipped with an objective heater and cells were examined in microscopy medium (137 mM NaCl, 5.4 mM KCl, 1.8 mM $CaCl_2$, 0.8 mM $MgSO_4$, 20 mM D-glucose and 20 mM HEPES) at 37°C.

Sample preparation for electron microscopy

Cell monolayers on round coverslips (12-mm diameter) were quickly washed in DMEM without FCS and fixed in situ with 4% paraformaldehyde in 0.1 M Sörensen phosphate buffer (pH 7.4) for 1 hour at 4°C. After washing at 4°C in the same buffer to remove unbound fixative, the specimens were dehydrated in increasing concentrations of ethanol and subsequently infiltrated with London Resin White (LR White, London Resin Company, Berkshire, England). Coverslips were attached to LR-White-resin-filled capsules and allowed to polymerize for 48 hours at 60°C. The embedded cells were separated from the coverslips by a short treatment with liquid nitrogen and cut parallel to the coverslip surface with a diamond knife using a Leica Ultracut UCT ultramicrotome. Ultrathin sections were mounted on Formvar-carbon-coated nickel grids (EMS, Warrington, PA) and processed for immunogold labeling or placed on uncoated gold grids for osmium ammine staining.

Immunogold labeling for electron microscopy

Ultrathin sections were pre-incubated on a drop of 1% normal goat serum (NGS, Nordic Immunology Laboratories, Tilburg, The Netherlands) in PBS for 3 minutes at room temperature. Incubation with anti-EGFP polyclonal primary antibodies diluted 1:100 in PBS containing 0.1% BSA (Fluka, Buchs, Switzerland) and 0.05% Tween 20 (Sigma-Aldrich, St Louis, MO) was carried out for 17 hours at 4°C in a humid chamber. After rinsing with PBS/Tween and incubating with PBS for 15 minutes, grids were treated again with NGS as above and labeled for 30 minutes at room temperature with colloidal gold-particle-conjugated secondary antibodies diluted in PBS. Detection of the polyclonal anti-EGFP Ab was done by incubating the grids with a goat anti-rabbit antibody (Aurion, Wageningen, The Netherlands) coupled with 15-nm colloidal gold particles (1:3 in PBS; Aurion, Wageningen, The Netherlands). Grids were finally rinsed with PBS and ultrapure water, and subsequently air-dried. For CPD detection, ultrathin sections were treated with 3 M HCl for 20 minutes at room temperature to denature dsDNA. After washing with water, sections were immunolabeled with a mouse monoclonal anti-CPD antibody (Kamiya Biomedical Company, Seattle, WA) diluted 1:800, using the protocol described above. Detection was carried out using a goat anti-mouse IgG antibody conjugated with 15-nm colloidal gold particles (Aurion) diluted 1:3 in PBS. As controls of labeling specificity, some grids were treated as above except that the primary antibody was omitted.

Most preparations were stained with the EDTA regressive technique, differential for nuclear nucleoprotein constituents (Bernhard, 1969), in a way that kept chromatin weakly contrasted. They were first stained with 5% uranyl acetate for 1 minute, then treated for 3 minutes with 0.02 M EDTA, and finally with lead citrate for 1 minute. To better evaluate whether there were differences in the chromatin area between the irradiated and non-irradiated cells, some thin sections were stained using a Feulgen-type reaction specific for DNA (Cogliati and Gautier, 1973). They were placed on uncoated gold grids, hydrolyzed with 5 N HCl for 20 minutes at room temperature, rinsed with distilled water and stained with 0.2% osmium ammine solution (saturated with SO_2) for 1 hour at room temperature. Electron micrographs were acquired with a Philips CM 12 or CM 10 electron microscope operating at 80 kV, using a 30- to 40-μm objective aperture.

Quantification of CPD and of NER protein distribution

To determine the nuclear distribution of CPDs and repair proteins, we quantified the signal obtained with anti-CPD antibodies and anti-EGFP antibodies as described above. Electron micrographs were acquired at a final magnification of ×31,000, using a CCD Morada camera (Olympus Soft Imaging System, Lakewood, CO). The signal in two nuclear regions was quantified: (1) condensed chromatin domains (CC) and (2) the perichromatin region (PR). The PR was operationally defined as a layer of 80-nm width, 40 nm on each side of the border of condensed chromatin domains. The labeling intensity of CPDs and repair proteins was expressed as the number of gold particles found in each subnuclear compartment per surface area of the cell nucleus (μm^2). This allows the averaging of data obtained for different nuclei. The surface area of the nucleus was determined morphometrically using NIH ImageJ 1.34 software (Office of Research Services, Bethesda, MD). The difference in surface area of condensed chromatin domains upon UV irradiation was quantified morphometrically also using NIH ImageJ software. The surface area of condensed chromatin domains was expressed as fraction of the surface area of the whole nucleus.

Estimating the expected accumulation of XPC in dense chromatin domains

The expression level of XPC-EGFP is similar to that of endogenous XPC in wild-type cells and is roughly 25,000 molecules (Araujo et al., 2001). About 20% of the nucleus is occupied by dense chromatin domains (Fig. 4), meaning that, if homogenously distributed, there will be ~5000 molecules in dense chromatin domains in non-irradiated cells. Global UV irradiation caused about 25% of the XPC-EGFP pool to be immobilized (Hoogstraten et al., 2008), corresponding to 6250 molecules that would accumulate in dense chromatin domains on top of the 5000 already present. Thus, the expected increase of XPC in dense chromatin domains is: (6250 + 5000)/5000 = 11,250/5000 = 2.25-fold increase. The measured increase in dense chromatin domains is about twofold, which corresponds well with the expected value.

The authors thank Jita Fakan and Francine Voinesco (Centre of Electron Microscopy, University of Lausanne) for their excellent technical assistance; Willy Blanchard for his photographic work; Liliane Hautle for helping in editing the manuscript; Martijn Moné and

Françoise Jaunin for initial experiments; and Federico Tessadori for critical reading of the manuscript. The authors acknowledge Joachim Goedhart (Swammerdam Institute for Life Sciences, University of Amsterdam, Amsterdam, The Netherlands) for technical assistance, and Erik Manders and Dorus Gadella for support. We are indebted to Jacques Rouquette for his kind help during the preparation of figures. This work was supported by the Swiss National Science Foundation (grant 3100AO-109333) and by the Netherlands Organisation for Health Research and Development (ZonMW, grant 912-03-012).

References

Araki, M., Masutani, C., Takemura, M., Uchida, A., Sugasawa, K., Kondoh, J., Ohkuma, Y. and Hanaoka, F. (2001). Centrosome protein centrin 2/caltractin 1 is part of the xeroderma pigmentosum group C complex that initiates global genome nucleotide excision repair. *J. Biol. Chem.* **276**, 18665-18672.

Araujo, S. J., Tirode, F., Coin, F., Pospiech, H., Syvaoja, J. E., Stucki, M., Hubscher, U., Egly, J. M. and Wood, R. D. (2000). Nucleotide excision repair of DNA with recombinant human proteins: definition of the minimal set of factors, active forms of TFIIH, and modulation by CAK. *Genes Dev.* **14**, 349-359.

Araujo, S. J., Nigg, E. A. and Wood, R. D. (2001). Strong functional interactions of TFIIH with XPC and XPG in human DNA nucleotide excision repair, without a preassembled repairosome. *Mol. Cell. Biol.* **21**, 2281-2291.

Balajee, A. S. and Bohr, V. A. (2000). Genomic heterogeneity of nucleotide excision repair. *Gene* **250**, 15-30.

Bernhard, W. (1969). A new staining procedure for electron microscopical cytology. *J. Ultrastruct. Res.* **27**, 250-265.

Bohr, V. A., Smith, C. A., Okumoto, D. S. and Hanawalt, P. C. (1985). DNA repair in an active gene: removal of pyrimidine dimers from the DHFR gene of CHO cells is much more efficient than in the genome overall. *Cell* **40**, 359-369.

Bouchet-Marquis, C., Dubochet, J. and Fakan, S. (2006). Cryoelectron microscopy of vitrified sections: a new challenge for the analysis of functional nuclear architecture. *Histochem. Cell Biol.* **125**, 43-51.

Brueckner, F. and Cramer, P. (2007). DNA photodamage recognition by RNA polymerase II. *FEBS Lett.* **581**, 2757-2760.

Buterin, T., Meyer, C., Giese, B. and Naegeli, H. (2005). DNA quality control by conformational readout on the undamaged strand of the double helix. *Chem. Biol.* **12**, 913-922.

Carrier, F., Georgel, P. T., Pourquier, P., Blake, M., Kontny, H. U., Antinore, M. J., Gariboldi, M., Myers, T. G., Weinstein, J. N., Pommier, Y. et al. (1999). Gadd45, a p53-responsive stress protein, modifies DNA accessibility on damaged chromatin. *Mol. Cell. Biol.* **19**, 1673-1685.

Cmarko, D., Verschure, P. J., Martin, T. E., Dahmus, M. E., Krause, S., Fu, X. D., van Driel, R. and Fakan, S. (1999). Ultrastructural analysis of transcription and splicing in the cell nucleus after bromo-UTP microinjection. *Mol. Biol. Cell* **10**, 211-223.

Cmarko, D., Verschure, P. J., Otte, A. P., van Driel, R. and Fakan, S. (2003). Polycomb group gene silencing proteins are concentrated in the perichromatin compartment of the mammalian nucleus. *J. Cell Sci.* **116**, 335-343.

Cogliati, R. and Gautier, A. (1973). Demonstration of DNA and polysaccharides using a new "Schiff type" reagent. *C. R. Hebd. Seances Acad. Sci., Ser. D, Sci. Nat.* **276**, 3041-3044.

Coin, F., Oksenych, V. and Egly, J. M. (2007). Distinct roles for the XPB/p52 and XPD/p44 subcomplexes of TFIIH in damaged DNA opening during nucleotide excision repair. *Mol. Cell* **26**, 245-256.

Cremer, T., Kupper, K., Dietzel, S. and Fakan, S. (2004). Higher order chromatin architecture in the cell nucleus: on the way from structure to function. *Biol. Cell* **96**, 555-567.

de Laat, W. L., Appeldoorn, E., Sugasawa, K., Weterings, E., Jaspers, N. G. and Hoeijmakers, J. H. (1998). DNA-binding polarity of human replication protein A positions nucleases in nucleotide excision repair. *Genes Dev.* **12**, 2598-2609.

de Laat, W. L., Jaspers, N. G. and Hoeijmakers, J. H. (1999). Molecular mechanism of nucleotide excision repair. *Genes Dev.* **13**, 768-785.

Dualan, R., Brody, T., Keeney, S., Nichols, A. F., Admon, A. and Linn, S. (1995). Chromosomal localization and cDNA cloning of the genes (DDB1 and DDB2) for the p127 and p48 subunits of a human damage-specific DNA binding protein. *Genomics* **29**, 62-69.

Fakan, S. (1994). Perichromatin fibrils are in situ forms of nascent transcripts. *Trends Cell Biol.* **4**, 86-90.

Fakan, S. (2004a). The functional architecture of the nucleus as analysed by ultrastructural cytochemistry. *Histochem. Cell Biol.* **122**, 83-93.

Fakan, S. (2004b). Ultrastructural cytochemical analyses of nuclear functional architecture. *Eur. J. Histochem.* **48**, 5-14.

Fakan, S. and van Driel, R. (2007). The perichromatin region: a functional compartment in the nucleus that determines large-scale chromatin folding. *Semin. Cell Dev. Biol.* **18**, 676-681.

Fitch, M. E., Nakajima, S., Yasui, A. and Ford, J. M. (2003). In vivo recruitment of XPC to UV-induced cyclobutane pyrimidine dimers by the DDB2 gene product. *J. Biol. Chem.* **278**, 46906-46910.

Fousteri, M., Vermeulen, W., van Zeeland, A. A. and Mullenders, L. H. (2006). Cockayne syndrome A and B proteins differentially regulate recruitment of chromatin remodeling and repair factors to stalled RNA polymerase II *in vivo*. *Mol. Cell* **23**, 471-482.

Fraschini, A., Pellicciari, C., Biggiogera, M. and Manfredi Romanini, M. G. (1981). The effect of different fixatives on chromatin: cytochemical and ultrastructural approaches. *Histochem. J.* **13**, 763-769.

Gazave, E., Gautier, P., Gilchrist, S. and Bickmore, W. A. (2005). Does radial nuclear organisation influence DNA damage? *Chromosome Res.* **13**, 377-388.

Giglia-Mari, G., Coin, F., Ranish, J. A., Hoogstraten, D., Theil, A., Wijgers, N., Jaspers, N. G., Raams, A., Argentini, M., van der Spek, P. J. et al. (2004). A new, tenth subunit of TFIIH is responsible for the DNA repair syndrome trichothiodystrophy group A. *Nat. Genet.* **36**, 714-719.

Green, C. M. and Almouzni, G. (2003). Local action of the chromatin assembly factor CAF-1 at sites of nucleotide excision repair *in vivo*. *EMBO J.* **22**, 5163-5174.

Groisman, R., Polanowska, J., Kuraoka, I., Sawada, J., Saijo, M., Drapkin, R., Kisselev, A. F., Tanaka, K. and Nakatani, Y. (2003). The ubiquitin ligase activity in the DDB2 and CSA complexes is differentially regulated by the COP9 signalosome in response to DNA damage. *Cell* **113**, 357-367.

Hanawalt, P. C. (2000). DNA repair: the bases for Cockayne syndrome. *Nature* **405**, 415-416.

Hanawalt, P. C. (2002). Subpathways of nucleotide excision repair and their regulation. *Oncogene* **21**, 8949-8956.

Hoeijmakers, J. H. (2001). Genome maintenance mechanisms for preventing cancer. *Nature* **411**, 366-374.

Hoogstraten, D., Nigg, A. L., Heath, H., Mullenders, L. H., van Driel, R., Hoeijmakers, J. H., Vermeulen, W. and Houtsmuller, A. B. (2002). Rapid switching of TFIIH between RNA polymerase I and II transcription and DNA repair *in vivo*. *Mol. Cell* **10**, 1163-1174.

Hoogstraten, D., Bergink, S., Verbiest, V. H., Luijsterburg, M. S., Geverts, B., Raams, A., Dinant, C., Hoeijmakers, J. H., Vermeulen, W. and Houtsmuller, A. B. (2008). Versatile DNA damage detection by the global genome nucleotide excision repair protein XPC. *J. Cell Sci.* **121**, 2850-2859.

Houtsmuller, A. B. and Vermeulen, W. (2001). Macromolecular dynamics in living cell nuclei revealed by fluorescence redistribution after photobleaching. *Histochem. Cell Biol.* **115**, 13-21.

Houtsmuller, A. B., Rademakers, S., Nigg, A. L., Hoogstraten, D., Hoeijmakers, J. H. and Vermeulen, W. (1999). Action of DNA repair endonuclease ERCC1/XPF in living cells. *Science* **284**, 958-961.

Hwang, B. J., Toering, S., Francke, U. and Chu, G. (1998). p48 Activates a UV-damaged-DNA binding factor and is defective in xeroderma pigmentosum group E cells that lack binding activity. *Mol. Cell. Biol.* **18**, 4391-4399.

Jaunin, F. and Fakan, S. (2002). DNA replication and nuclear architecture. *J. Cell Biochem.* **85**, 1-9.

Jaunin, F., Visser, A. E., Cmarko, D., Aten, J. A. and Fakan, S. (2000). Fine structural in situ analysis of nascent DNA movement following DNA replication. *Exp. Cell Res.* **260**, 313-323.

Kruhlak, M. J., Celeste, A., Dellaire, G., Fernandez-Capetillo, O., Muller, W. G., McNally, J. G., Bazett-Jones, D. P. and Nussenzweig, A. (2006). Changes in chromatin structure and mobility in living cells at sites of DNA double-strand breaks. *J. Cell Biol.* **172**, 823-834.

Kuo, W. H., Wang, Y., Wong, R. P., Campos, E. I. and Li, G. (2007). The ING1b tumor suppressor facilitates nucleotide excision repair by promoting chromatin accessibility to XPA. *Exp. Cell Res.* **313**, 1628-1638.

Laine, J. P. and Egly, J. M. (2006). When transcription and repair meet: a complex system. *Trends Genet.* **22**, 430-436.

Lehmann, A. R., Niimi, A., Ogi, T., Brown, S., Sabbioneda, S., Wing, J. F., Kannouche, P. L. and Green, C. M. (2007). Translesion synthesis: Y-family polymerases and the polymerase switch. *DNA Repair (Amst.)* **6**, 891-899.

Lindahl, T. and Wood, R. D. (1999). Quality control by DNA repair. *Science* **286**, 1897-1905.

Luijsterburg, M. S., Goedhart, J., Moser, J., Kool, H., Geverts, B., Houtsmuller, A. B., Mullenders, L. H., Vermeulen, W. and van Driel, R. (2007). Dynamic *in vivo* interaction of DDB2 E3 ubiquitin ligase with UV-damaged DNA is independent of damage-recognition protein XPC. *J. Cell Sci.* **120**, 2706-2716.

Maillard, O., Solyom, S. and Naegeli, H. (2007). An aromatic sensor with aversion to damaged strands confers versatility to DNA repair. *PLoS Biol.* **5**, e79.

Mellon, I., Spivak, G. and Hanawalt, P. C. (1987). Selective removal of transcription-blocking DNA damage from the transcribed strand of the mammalian DHFR gene. *Cell* **51**, 241-249.

Missura, M., Buterin, T., Hindges, R., Hubscher, U., Kasparkova, J., Brabec, V. and Naegeli, H. (2001). Double-check probing of DNA bending and unwinding by XPA-RPA: an architectural function in DNA repair. *EMBO J.* **20**, 3554-3564.

Mitchell, D. L. and Nairn, R. S. (1989). The biology of the (6-4) photoproduct. *Photochem. Photobiol.* **49**, 805-819.

Mori, T., Nakane, M., Hattori, T., Matsunaga, T., Ihara, M. and Nikaido, O. (1991). Simultaneous establishment of monoclonal antibodies specific for either cyclobutane pyrimidine dimer or (6-4)photoproduct from the same mouse immunized with ultraviolet-irradiated DNA. *Photochem. Photobiol.* **54**, 225-232.

Moser, J., Volker, M., Kool, H., Alekseev, S., Vrieling, H., Yasui, A., van Zeeland, A. A. and Mullenders, L. H. (2005). The UV-damaged DNA binding protein mediates efficient targeting of the nucleotide excision repair complex to UV-induced photo lesions. *DNA Repair (Amst.)* **4**, 571-582.

Moser, J., Kool, H., Giakzidis, I., Caldecott, K., Mullenders, L. H. and Fousteri, M. I. (2007). Sealing of chromosomal DNA nicks during nucleotide excision repair requires XRCC1 and DNA ligase III alpha in a cell-cycle-specific manner. *Mol. Cell* **27**, 311-323.

Mullenders, L. H. and Berneburg, M. (2001). Photoimmunology and nucleotide excision repair: impact of transcription coupled and global genome excision repair. *J. Photochem. Photobiol. B, Biol.* **65**, 97-100.

Murga, M., Jaco, I., Fan, Y., Soria, R., Martinez-Pastor, B., Cuadrado, M., Yang, S. M., Blasco, M. A., Skoultchi, A. I. and Fernandez-Capetillo, O. (2007). Global chromatin compaction limits the strength of the DNA damage response. *J. Cell Biol.* **178**, 1101-1108.

Polo, S. E., Roche, D. and Almouzni, G. (2006). New histone incorporation marks sites of UV repair in human cells. *Cell* **127**, 481-493.

Rademakers, S., Volker, M., Hoogstraten, D., Nigg, A. L., Moné, M. J., Van Zeeland, A. A., Hoeijmakers, J. H., Houtsmuller, A. B. and Vermeulen, W. (2003). Xeroderma pigmentosum group A protein loads as a separate factor onto DNA lesions. *Mol. Cell. Biol.* **23**, 5755-5767.

Rubbi, C. P. and Milner, J. (2003). p53 is a chromatin accessibility factor for nucleotide excision repair of DNA damage. *EMBO J.* **22**, 975-986.

Shivji, M. K., Eker, A. P. and Wood, R. D. (1994). DNA repair defect in xeroderma pigmentosum group C and complementing factor from HeLa cells. *J. Biol. Chem.* **269**, 22749-22757.

Sugasawa, K., Ng, J. M., Masutani, C., Iwai, S., van der Spek, P. J., Eker, A. P., Hanaoka, F., Bootsma, D. and Hoeijmakers, J. H. (1998). Xeroderma pigmentosum group C protein complex is the initiator of global genome nucleotide excision repair. *Mol. Cell* **2**, 223-232.

Takao, M., Abramic, M., Moos, M., Jr, Otrin, V. R., Wootton, J. C., McLenigan, M., Levine, A. S. and Protic, M. (1993). A 127 kDa component of a UV-damaged DNA-binding complex, which is defective in some xeroderma pigmentosum group E patients, is homologous to a slime mold protein. *Nucleic Acids Res.* **21**, 4111-4118.

Tang, J. Y., Hwang, B. J., Ford, J. M., Hanawalt, P. C. and Chu, G. (2000). Xeroderma pigmentosum p48 gene enhances global genomic repair and suppresses UV-induced mutagenesis. *Mol. Cell* **5**, 737-744.

van Hoffen, A., Venema, J., Meschini, R., van Zeeland, A. A. and Mullenders, L. H. (1995). Transcription-coupled repair removes both cyclobutane pyrimidine dimers and 6-4 photoproducts with equal efficiency and in a sequential way from transcribed DNA in xeroderma pigmentosum group C fibroblasts. *EMBO J.* **14**, 360-367.

Volker, M., Moné, M. J., Karmakar, P., van Hoffen, A., Schul, W., Vermeulen, W., Hoeijmakers, J. H., van Driel, R., van Zeeland, A. A. and Mullenders, L. H. (2001). Sequential assembly of the nucleotide excision repair factors *in vivo*. *Mol. Cell* **8**, 213-224.

Wang, J., Chin, M. Y. and Li, G. (2006). The novel tumor suppressor p33ING2 enhances nucleotide excision repair via inducement of histone H4 acetylation and chromatin relaxation. *Cancer Res.* **66**, 1906-1911.

Yokoi, M., Masutani, C., Maekawa, T., Sugasawa, K., Ohkuma, Y. and Hanaoka, F. (2000). The xeroderma pigmentosum group C protein complex XPC-HR23B plays an important role in the recruitment of transcription factor IIH to damaged DNA. *J. Biol. Chem.* **275**, 9870-9875.

Ziv, Y., Bielopolski, D., Galanty, Y., Lukas, C., Taya, Y., Schultz, D. C., Lukas, J., Bekker-Jensen, S., Bartek, J. and Shiloh, Y. (2006). Chromatin relaxation in response to DNA double-strand breaks is modulated by a novel ATM- and KAP-1 dependent pathway. *Nat. Cell Biol.* **8**, 870-876.

Zotter, A., Luijsterburg, M. S., Warmerdam, D. O., Ibrahim, S., Nigg, A., van Cappellen, W. A., Hoeijmakers, J. H., van Driel, R., Vermeulen, W. and Houtsmuller, A. B. (2006). Recruitment of the nucleotide excision repair endonuclease XPG to sites of UV-induced dna damage depends on functional TFIIH. *Mol. Cell. Biol.* **26**, 8868-8879.

Journal of Cell Science